



# Thermal Performance Study of Parallel and Radial Divergence Microchannel Arrangement Using Numerical Method

Sahib Shihab Ahmed <sup>1,\*</sup>, Abdul Muhsin A. Rageb <sup>2</sup>

<sup>1</sup>Department of Mechanical Engineering, College of Engineering, University of Kufa, Najaf, Iraq  
<sup>2</sup>Department of Mechanical Engineering, College of Engineering, University of Basrah, Basrah, Iraq  
 E-mail address: [sahib.aldulaimi@uokufa.edu.iq](mailto:sahib.aldulaimi@uokufa.edu.iq), [muhsinrageb@yahoo.ie](mailto:muhsinrageb@yahoo.ie)  
 Received: 1 December 2019; Accepted: 22 December 2019; Published: 2 February 2020

## Abstract

In the present study, a three dimensional simulations of the single phase laminar flow and forced convection heat transfer of water in the five layers of microchannel heat sink with both arrangement radial and a parallel divergence channel have been studied numerically. The thermal characteristics and pressure drop of the heat sink were investigated for same mass flow rate ( $3.925 \times 10^{-4}$  kg/s) and constant heat flux ( $90 \text{ W/cm}^2$ ). The results obtained show that, using of the radial microchannel led to improve both the hydrodynamic and thermal performance of heat sink. It led to reduce the pressure drop by 32.5 % and increase the performance index about 1.5 compared with the parallel divergence microchannel heat sink also it gives better temperature uniformity.

© 2020 The Authors. Published by the University of Basrah. Open-access article.

**Keywords:** Radial heat sink, microchannel, performance index, temperature uniformity.

## 1. Introduction

A heat sink is an electronic device made of good thermal conducting material and usually attached to an electronic device to dissipate the unwanted heat. The fast development of computing technology has led to the reduction and density integration to electronic devices which involves more heat generation per unit area [1]. Microchannel was considered as innovative cooling technology of removal an excessive that heat flux from minor regions. Their features make it have many applications in cooling in high power electronic plans, aerospace, heat exchanger, combustor, gas absorbers, and solvent extractors [2]. The advanced cooling technology using micro channels were first proposed by Tuckerman and Pease [3] they used silicon microchannel with single phase of water as working fluid to dissipate heat from a chip. The results noticed that maximum wall sink temperature growth to  $71^\circ\text{C}$  beyond the inlet water temperature. They concluded that the maximum power heat flux could be dissipated using the microchannels was  $790 \text{ W/cm}^2$ . Qu and Mudawar [4] numerically analyzed three dimension fluid flow and heat transfer of rectangular microchannel heat sink using water as cooling fluid. Their results showed that increasing the thermal conductivity of the solid substrate reduces the

temperature oh the heat sink. Duryodhan et al. [5] experimentally studied fluid flow characteristics inside diverging microchannel. They investigated the influence of mass flow rate, diverging angle and length on pressure were investigated. Their results showed that the pressure drop has a linear dependency with mass flow rate and inversely with the divergence angle. Duryodhan et al. [6] studied experimentally and numerically of the liquid flow through converging microchannel. They presented a comparison of fluid flow in converging and diverging microchannel. They observed that the pressure drop varied non-linearly with the volume flow rate. Yu et al. [7] studied numerically and experimentally the natural convection with rectangular fins mounted radially. The influence of fin height, their number and length were investigated. Their results showed that main factor were inversely proportional to evacuation rate. Hassan et al. [8] investigated the thermal performance of a radial micro heat exchanger with varying diverging channel. They studied two models firstly, using (1-D) thermal resistance based model and secondly utilizing (3-D) CFD model. The results found to have thermal performance that was equivalent to or better than performance other microchannel heat sink. Roy et al. [9] summarized the recent advances in the area of fluid flow and heat transfer applications in radially rotating micro channels. Ghaedamini et al. [10] studied convective cooling of a circular disc by using radial and dendritic microchannel. The contribution of the cross section area in radial designs was investigated by varying its height. Their results showed that a reduction in height lead to decrease in thermal resistance, but the pressure drop increase. Xu et al. [11] studied experimentally and numerically of the heat transfer performance of a symmetrical fractal microchannel network subjected to pulsation flow. They investigated the influences of pulsation frequency on the pressure drop, temperature and Nusselt number. Their results displayed that the pulsation flow through fractal like microchannel provides reduce maximum temperature and a better cooling capacity.

The main objective of the present work is to compare the performance of a radial microchannel heat sink with the parallel divergent microchannel of rectangular cross section heat sink. Two arrangements for same volume of heat sink, same total mass flow rate, and same area subjected to the constant heat flux and same aspect ratio of inlet and outlet



were numerically investigated. Furthermore, using of the radial microchannel are alternatives to the parallel divergence microchannel heat sink with goal of lessening the pressure drop, that enchaining heat transfer.

## 2. Model Description

Two arrangements of microchannel heat sinks of same volume have been used in this work. First arrangement consists of a five layers stack of horizontal parallel divergent microchannel which divergent from sides, each layer contains (107) microchannel. The dimensions of parallel divergent microchannel are a fixed height  $H_{ch}$ , fixed width at inlet  $W_{in}$ , wall thickness separating two channels  $W_w$  and length of channel  $L_{ch}$  as shown in Figs. 1 (a), (b), (c). The width of the channels is changed with the divergence angles ( $\varphi$ ) and its height still constant defined by:

$$W_{out} = W_{in} + 2 \times L_{ch} \times \tan \varphi \tag{1}$$

A radially microchannel heat sink was designed using similar criterion (volume, mass flow rate and heat flux) as the parallel divergent heat sink. Second arrangement consists of a five layers of horizontal radial microchannel, each layer contains (157) microchannel, which depended on angle ( $\beta$ ). A one radial microchannel consists of a fixed height  $H_{ch}$ , fixed width at inlet  $W_{in}$ , fixed wall thickness separating two channels  $W_w$ , length of channel  $L_{ch}$ , which spans the inner  $R_i$  (6000  $\mu\text{m}$ ) to outer  $R_o$  (16000  $\mu\text{m}$ ) radius as shown in Figs. 2 (a), (b), (c). The width at outlet  $W_{out}$ , which depended on angle of divergence ( $\theta_{ch}$ ) and equal to  $W_{out}$  of first arrangement and can define by:

$$W_{out} = R_o \times \theta_{ch} \tag{2}$$

The dimensions of heat sink are presented in Table 1. The aspect ratio defined by:

$$\alpha = \frac{W_{ch}}{H_{ch}} \tag{3}$$

**Table 1** dimension of the heat sinks for both arrangements (the radial and parallel divergence).

Dimension	Rectangular	Radial
$W/R_i, R_o$	6.9 mm	6 mm, 16 mm
$H$	1.2 mm	1.2 mm
$L_{ch}$	10 mm	10 mm
$W_{in}$	100 $\mu\text{m}$	100 $\mu\text{m}$
$H_{ch}$	100 $\mu\text{m}$	100 $\mu\text{m}$
$W_w$	70 $\mu\text{m}$	70 $\mu\text{m}$
$W_{out}$	70 $\mu\text{m}$	70 $\mu\text{m}$

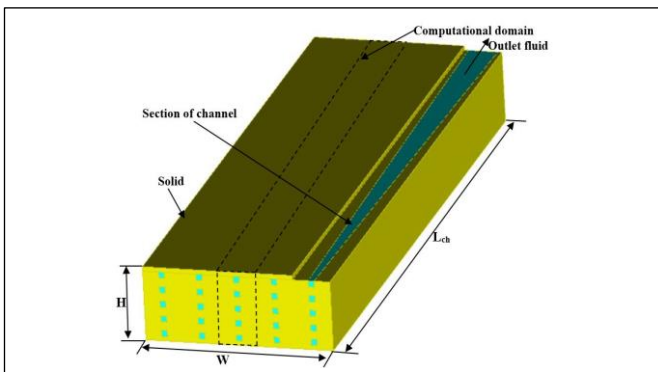


**Fig. 1 (a)** the parallel divergent rectangular heat sinks.

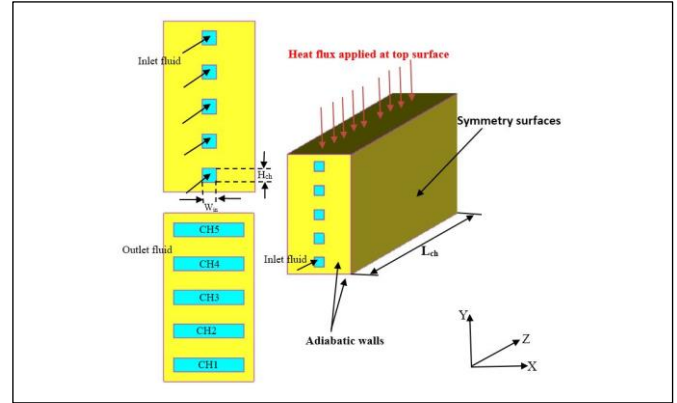


**Fig. 1 (b)** Computational domain of the parallel divergent microchannel.

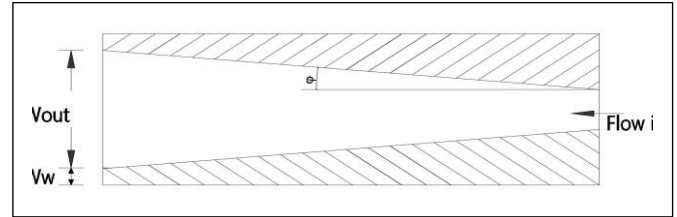


**Fig. 1 (c)** Parallel divergent microchannel (top view section).

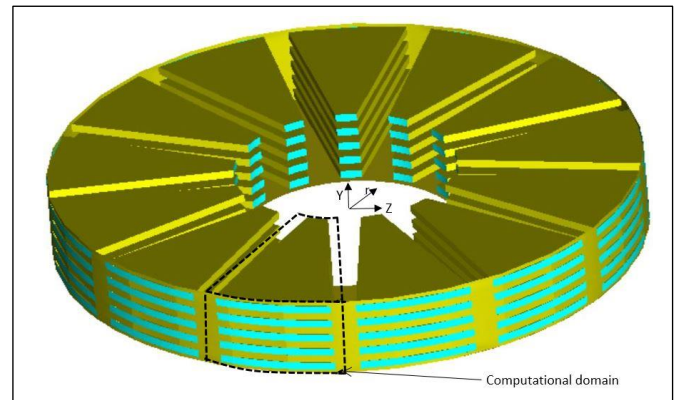


**Fig. 2 (a)** the radial heat sinks.

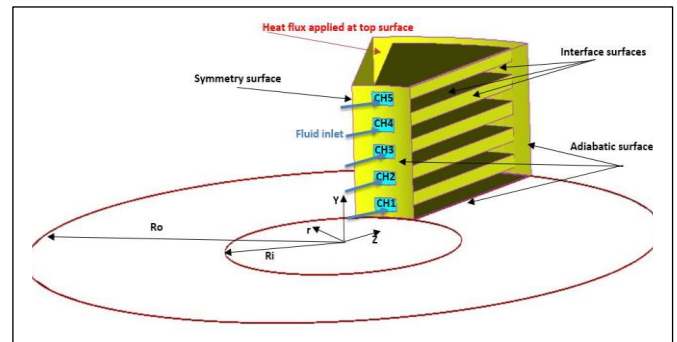


**Fig. 2 (b)** Computational domain of the radial microchannel.

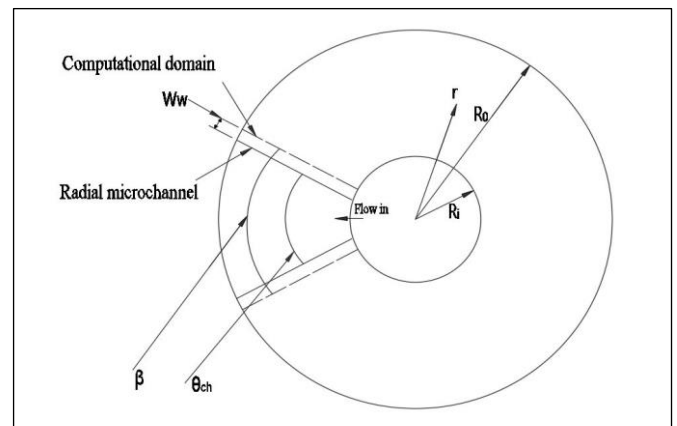


**Fig. 2 (c)** Radial microchannel with heat sink (top view).

### 3. Governing Equations

To simplify the fluid flow and heat transfer analysis, the flow is assumed as steady-state, three-dimensional, laminar, nonslip flow, and incompressible. The radiation and gravitational effects were neglected. According to the above assumptions, the governing equations can be expressed as follows [12]:

Continuity equation:

$$\rho \left( \frac{\partial u}{\partial x} + \frac{\partial v}{\partial y} + \frac{\partial w}{\partial z} \right) = 0 \quad (4)$$

Momentum equation:

X- Direction

$$\rho \left( u \frac{\partial u}{\partial x} + v \frac{\partial u}{\partial y} + w \frac{\partial u}{\partial z} \right) = -\frac{\partial P}{\partial x} + \mu \left( \frac{\partial^2 u}{\partial x^2} + \frac{\partial^2 v}{\partial y^2} + \frac{\partial^2 w}{\partial z^2} \right) \quad (5)$$

Y- Direction

$$\rho \left( u \frac{\partial v}{\partial x} + v \frac{\partial v}{\partial y} + w \frac{\partial v}{\partial z} \right) = -\frac{\partial P}{\partial y} + \mu \left( \frac{\partial^2 v}{\partial x^2} + \frac{\partial^2 v}{\partial y^2} + \frac{\partial^2 v}{\partial z^2} \right) \quad (6)$$

Z- Direction

$$\rho \left( u \frac{\partial w}{\partial x} + v \frac{\partial w}{\partial y} + w \frac{\partial w}{\partial z} \right) = -\frac{\partial P}{\partial z} + \mu \left( \frac{\partial^2 w}{\partial x^2} + \frac{\partial^2 w}{\partial y^2} + \frac{\partial^2 w}{\partial z^2} \right) \quad (7)$$

Energy equation:

$$\rho c_p \left( u \frac{\partial T}{\partial x} + v \frac{\partial T}{\partial y} + w \frac{\partial T}{\partial z} \right) = k \left( \frac{\partial^2 T}{\partial x^2} + \frac{\partial^2 T}{\partial y^2} + \frac{\partial^2 T}{\partial z^2} \right) \quad (8)$$

The energy equation for solid is written as:

$$k \left( \frac{\partial^2 T}{\partial X^2} + \frac{\partial^2 T}{\partial Y^2} + \frac{\partial^2 T}{\partial Z^2} \right) = 0 \quad (9)$$

### 4. Boundary Conditions

Water was used as the working fluid in the microchannel with uniform velocity at inlet. Silicon was taken as the material of the heat sink. The boundary conditions used are:

#### 4. 1. For fluid

At the channel inlet:

$$\text{At } z = 0, V = V_{in} \text{ and } T = T_{in}$$

At the channel exit:

$$\text{At } z = L_{ch}, \quad \frac{\partial u}{\partial z} = \frac{\partial v}{\partial z} = \frac{\partial w}{\partial z} = 0, \quad \frac{\partial T}{\partial z} = 0$$

At inner walls of the channels, the conjugate (fluid - solid interface) heat transfer boundary and no slip conditions are imposed:

$$u = v = w = 0, -k_f \frac{\partial T_f}{\partial n} = -k_s \frac{\partial T_s}{\partial n} \text{ and } T_f = T_s$$

#### 4. 2. For solid walls

The adiabatic boundary was used at all outer sides of solid walls except top wall was subjected to constant heat flux.

Where,

$$\text{At } y = H, q'' = \text{constant} = -k_s \frac{\partial T_s}{\partial y}$$

### 5. Solution Procedure

A finite volume method (FVM) is used to convert governing equations to algebraic equations accomplished using an upwind scheme. The SIMPLE algorithm is used to enforce mass conservation and to obtain the pressure field. The segregated solver is used to solve the governing integral equations for the conservation of mass, momentum and energy [13]. The convergence criteria to control the solution for momentum and energy equation were set to be less than  $10^{-6}$ .

### 6. Thermal parameters

The numerical computation is carried out by solving the governing conservation equations according to the boundary conditions using numerical program and the pressure, the distribution of velocity, the distribution of temperature and other required parameters were calculated. The value of Nusselt number is computed based on the local values of heat transfer coefficient ( $h$ ) and defined as [14]:

$$Nu = \frac{q'' D_h}{k_f (T_w - T_b)} \quad (10)$$

Where,

$$D_h = \frac{2(H_{ch} W_{in})}{(H_{ch} + W_{in})}$$

And  $T_w$  is the local average temperature of wall is given by:

$$T_w = \frac{\int T dA_c}{\int dA_c} \quad (11)$$

Fluid bulk temperature can be calculated from:

$$T_b = \frac{\int u T dA_c}{\int u dA_c} \quad (12)$$

The value of  $\overline{Nu}$  is obtained by integrating the local  $Nu$  along channel by using trapezoidal rule [13]:

$$\overline{Nu} = \frac{1}{A} \int_0^A Nu dA \quad (13)$$

$$\overline{Nu} = \frac{\Delta Z}{2L} \left( Nu_{z=0} + Nu_{z=L} + 2 \sum_{i=2}^N Nu_{z=i} \right) \quad (14)$$

The performance index is a ratio of average Nusselt number to the pressure drop along the heat sink, it gives an indication about the overall performance of a microchannel heat sink (MCHS) including both the hydrodynamic and thermal performance and defined by [15]:

$$\text{performance index (PI)} = \frac{\overline{Nu}}{\Delta p} \quad (15)$$

The heat transfer enhancement ratio (HTER) is used to compare the heat transfer and pressure drop as defined by [15]:

$$HTER = \frac{(PI)_{radial}}{(PI)_{rectangular}} \quad (16)$$

While the temperature difference (temperature uniformity) for wall of heat sink defined as [16]:

$$\Delta T = T_{max} - T_{min} \quad (17)$$

## 7. Grid Dependency Test

The grid dependent test is first conducted by using several different mesh sizes. ICEM CFD commercial mesh generator software is used to generate the numerical mesh domain. A hexahedral unstructured element was used as shown in Fig. 3. The governing equations were resolved based on these four meshes. The results obtained from these meshes at mass flow rate =  $0.5 \times 10^{-6}$  kg/s are summarized in Table 2, which shows the number of nodes used, fluid bulk temperature at outlet and pressure drop. From these results it can be seen that the solution becomes independent of grid size and increasing the size of mesh more than the third one (60, 220, 150) do not have important effect on the results just increasing the run time and memory requirements. Therefore, the third mesh will be considered in the next calculations.

Table 2 Grid dependent test.

No.	Mesh size (W, H, L)	Bulk temperature (K)	Pressure drop (Pa)
1	(30, 110, 100)	328.33429	4100.995971
2	(50, 160, 150)	328.35121	4329.24968
3	(60, 220, 150)	328.35954	4306.210424
4	(70, 270, 200)	328.35962	4306.211630

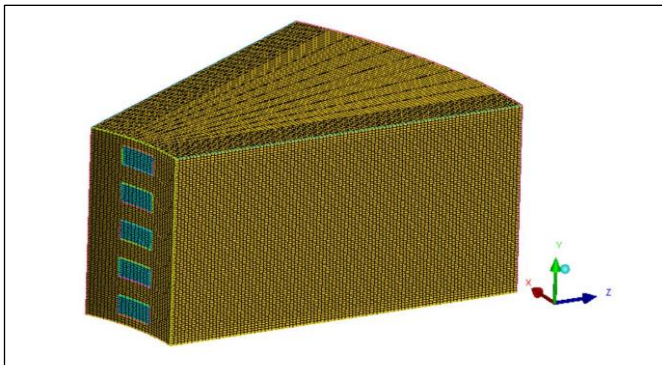


Fig. 3 Mesh of discretized of computational domain.

## 8. Code Validation

To check the precision of the current numerical simulation, verification was had been made by comparing the numerical results of current simulation with the numerical results of Qu and Mudawar [4]. The numerical model present in Qu and Mudawar [4] is a microchannel heat sink has a width of  $57 \times 10^{-3}$  mm, depth  $180 \times 10^{-3}$  mm and  $43 \times 10^{-3}$  mm width of wall separated between channels. Same boundary conditions were used to resolve the governing equations, a get excellent agreement obtain between the present work and that work by Qu and Mudawar [4] as shown in Fig. 4.

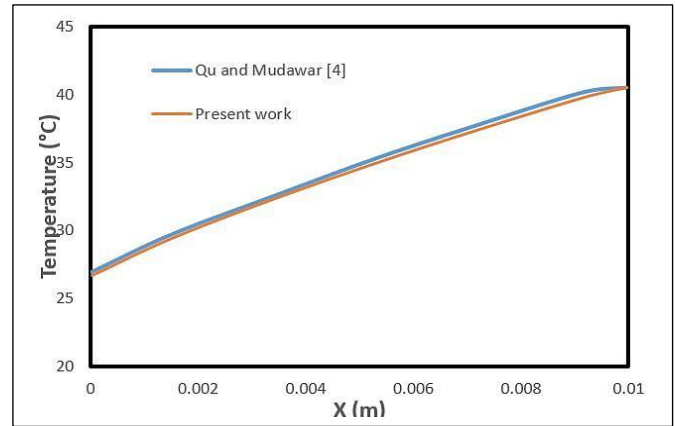


Fig. 4 Comparison of temperature of present numerical study with Qu and Mudawar model [4].

## 9. Results and Dissection

In order to check the validation of the results, simulation result has been compared with experimental result. The experimental work presented in Duryodhan et al. [6] was a microchannel heat sink consists of converging rectangular microchannel with hydraulic diameter  $147 \mu\text{m}$ , channel height  $78 \mu\text{m}$ , minimum width  $211 \mu\text{m}$ , angle of converging  $8^\circ$  and channel length 20 mm. Fig. 5 shows the comparison of the pressure drop between results of present numerical simulation and the experimental data of Duryodhan et al. [6]. It can be seen from this figure the agreement between experimental results and numerical simulation is excellent since the maximum error is 1.51 %. Therefore, the present numerical model is reliable and can be rightly used to do the numerical simulation. In present work a five layers of the radial microchannel were numerically studied and compared to a parallel divergence microchannel with an inlet and outlet aspect ratio of 1 and 5 respectively. Fig. 6 shows a comparison of the average wall temperature distribution between parallel divergence microchannel and radial microchannel along flow direction for same mass flow rate. From this figure it can be noticed that wall temperature increased along the channels length due to the applied heat flux continuously along the heat sink for both cases. The average wall temperature of a radial channel was less than a parallel divergence channel for all channels except CH5 it increase at the end channel as maximum percentage 0.1 % because distribution of channels. In Fig. 7 variation bulk temperature along channel length for the radial microchannel and parallel divergence microchannel, from this figure it can be observed the bulk temperature for radial channel is less than parallel divergence microchannel because increase of number of channels in the radial heat sink. The variations of walls temperature distribution (top walls, bottom walls and side walls) of the radial heat sink and parallel divergence heat sink with flow direction can be seen in Fig. 8. This figure indicates that the temperature of all walls of radial heat sink is less than parallel divergence heat sink except the end of top wall because decrease heat transfer due to decrease in surface area in the radial arrangement. Fig. 9 shows the average of walls temperature distribution for both the radial heat sink and parallel divergence heat sink with flow direction. From this figure it's clear that the average wall temperature of parallel divergence heat sink is higher than of the radial heat sink because of radial microchannel occupies nearly whole empty solid space between channels, it is best arrangement than parallel divergence. The variation of pressure drop  $\Delta P$



along channel length for both cases can be seen in Fig. 10. From this figure can be noticed the pressure drop of the parallel divergence microchannel greater than the radial microchannel because arrangement of channels lead to decrease number of channels in parallel divergence heat sink and increase mass flow rate for one parallel divergent rectangular microchannel. Effect of channel arrangement (parallel divergent microchannel and radial microchannel) on average Nusselt number ( $Nu$ ) for CH5 with flow direction can be seen in Fig. 11. It can be concluded the ( $Nu$ ) of radial arrangement microchannel is greater than parallel divergence microchannel because of the radial distribution of channels, most of the solid regions are occupied nearly leads to uniformity of heat flux more. Fig. 12 represents the performance index ( $PI$ ) of CH5 along channel length for the two cases. From figure it can be noticed that radial microchannel gives the best value of average Nusselt number on pressure drop (which favorite to heat sink design) because the average Nusselt number of radial microchannel is high and pressure drop is less than parallel divergence as shown in Figs. 10 and 11. From Table 3, it can be showed that the using of radial microchannels leads to increases the performance index by 1.5 compare to the parallel divergence microchannel since the distribution of divergent microchannel in the radially are more suitable and led to increase number of microchannel causes a decrease in mass flow rate in channels, and thus leads to decrease pressure drop. Also temperature uniformity of the radial microchannel is less than the parallel divergence microchannel as shown in Table 4.

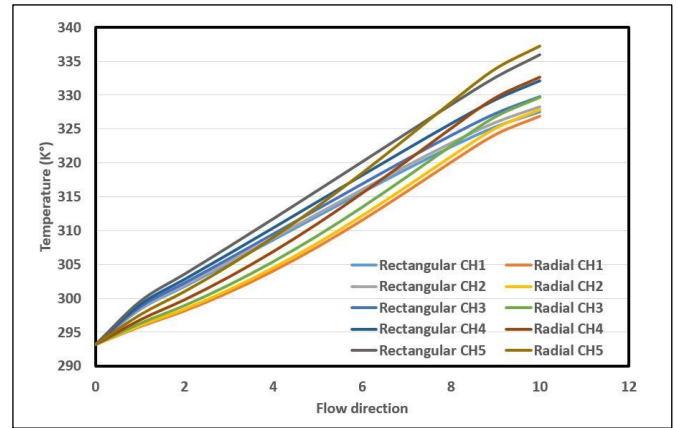


Fig. 7 Bulk temperature variations of all parallel divergent and radial microchannel.

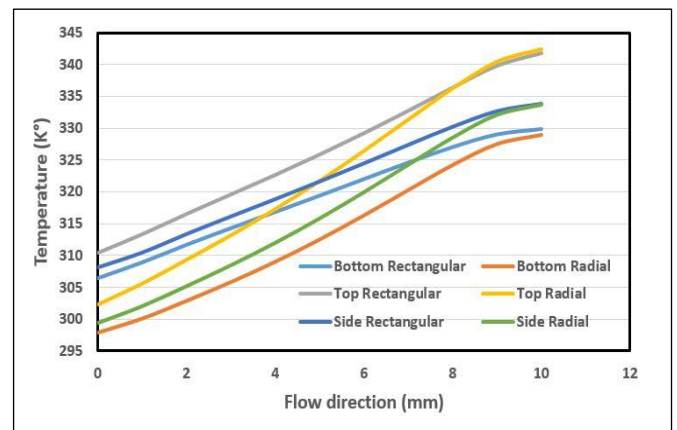


Fig. 8 Wall temperature of parallel divergent and radial microchannel heat sink.

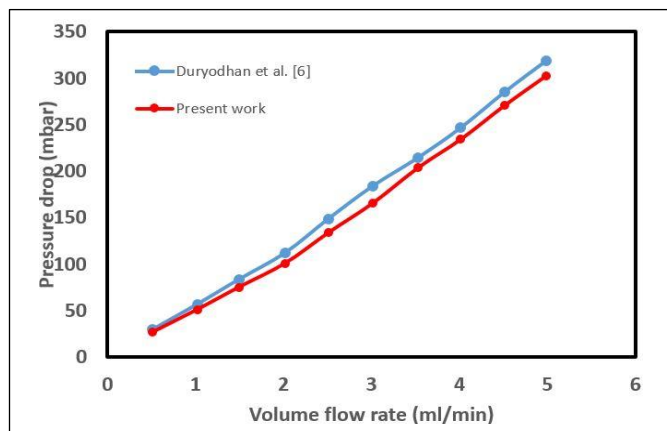


Fig. 5 Comparison of pressure drops of present numerical study with previous studies.

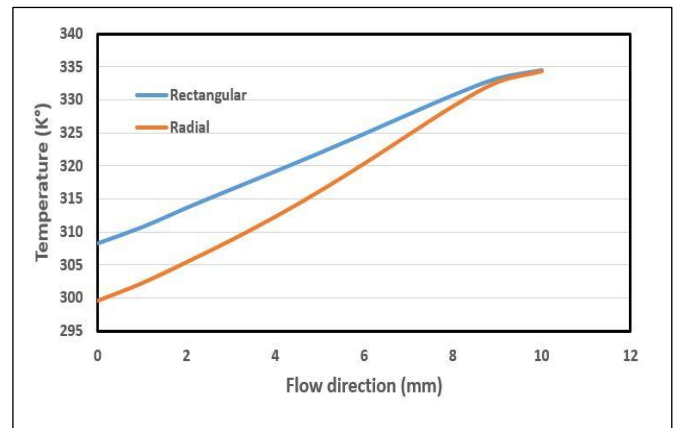


Fig. 9 Average wall temperature of parallel divergent and radial microchannel heat sink.

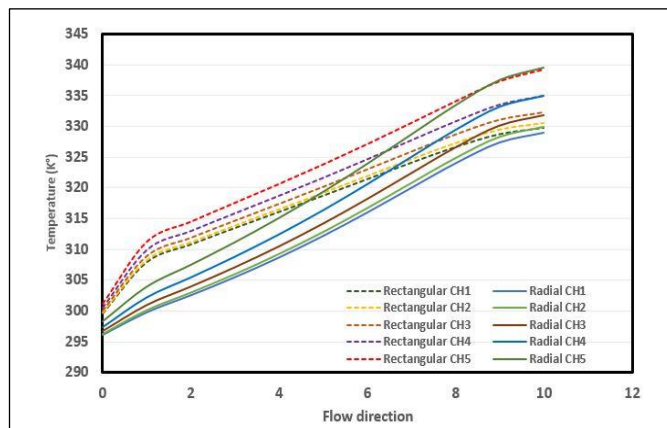


Fig. 6 Average wall temperature variations of all parallel divergent and radial microchannel.

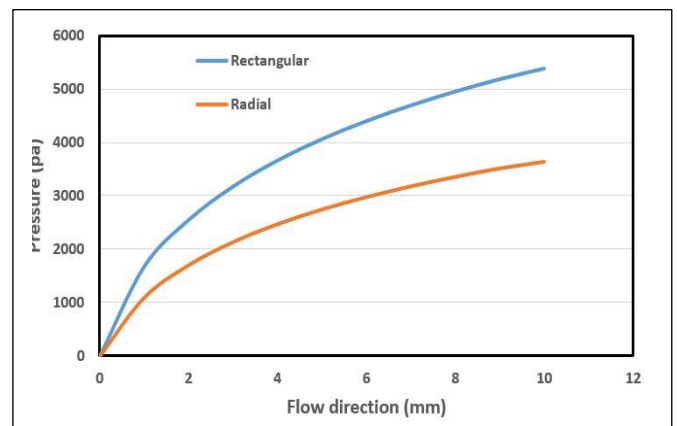


Fig. 10 Pressure drop of parallel divergent and radial microchannel (CH5).

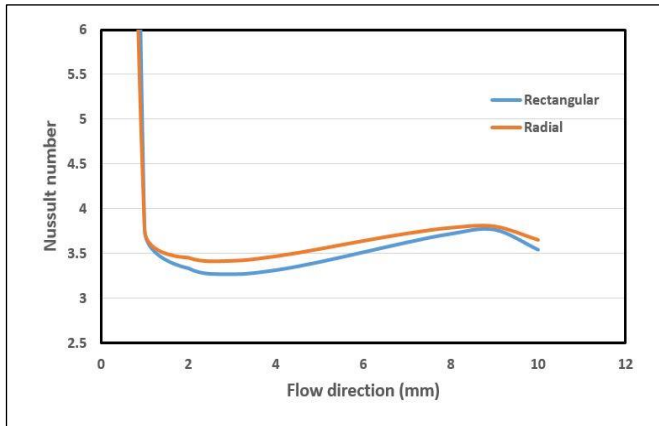


Fig. 11 Average Nusselt number of parallel divergent and radial microchannel (CH5).

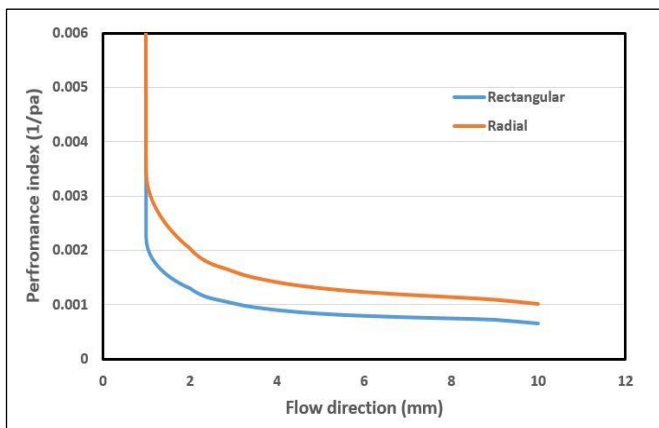


Fig. 12 Performance index of parallel divergent and radial microchannel (CH5).

Table 3 Heat transfer effect ratio (HTER).

Channels	CH1	CH2	CH3	CH4	CH5
HTER	1.55	1.554	1.548	1.541	1.533

Table 4 Temperature uniformity.

Channels	CH1	CH2	CH3	CH4	CH5
$\Delta T$ radial	35.722	36.707	38.696	41.731	46.138
$\Delta T$ parallel	36.618	37.439	39.122	41.757	46.086

## 10. Conclusions

The numerical simulation in this paper is made to study the effect of distribution of divergence microchannel. The rearrangement of the microchannel have been studied for two cases (parallel divergent and radial) to find best performance and distribution. From the results obtained the following conclusions can be draw:

1. The distribution of the radial micro channels is best than parallel divergence and the radial micro channels took advantage of the empty space between the micro channels.
2. Using the radial microchannel heat sink lead to reduce the pressure drop from parallel divergence microchannel heat sink about 32.5 %.
3. The value of heat transfer enhancement ratio (HTER) of the radial microchannel found to be increased reach to 1.5 compared to that the parallel divergence microchannel.
4. The radial microchannel caused improvement in Nussult number compared to the parallel divergence microchannel.

5. The temperature uniformity of the radial microchannel arrangement is improved compared to parallel divergence microchannel.

## References

- [1] M. R. Salimpour, M. Sharifhasan, and E. Shirani, "Constructal optimization of microchannel heat sinks with noncircular cross sections", *Heat Transfer Engineering*, Vol. 34, No. 10, pp. 863-874, 2013.
- [2] Ben-Ran Fu, "Liquid-liquid mixtures flow in microchannels", *Transactions of the Canadian Society for Mechanical Engineering*, Vol. 37, No. 3, pp. 631-640, 2013.
- [3] D. B. Tuckerman and R. F. W. Pease, "High-Performance Heat Sinking for VLSI", Vol. 2, Issue 5, pp. 126-129, 1981.
- [4] Weilin Qu and Issam Mudawar, "Analysis of three-dimensional heat transfer in micro-channel heat sinks", Vol. 45, Issue 19, pp. 3973-3985, 2002.
- [5] V. S. Duryodhan, S. G. Singh, and Amit Agrawal, "Liquid flow through a diverging microchannel", *Springer, Microfluid. Nanofluidics*, Vol. 14, Issue 1-2, pp. 53-67, 2013.
- [6] V. S. Duryodhan, S. G. Singh, and A. Agrawal, "Liquid flow through converging microchannels and a comparison with diverging microchannels", *Journal of Micromechanics and Microengineering*, Vol. 24, No. 12, pp. 1-13, 2014.
- [7] Seunghwan H. Yu, Kwan-Soo Lee, and Se-Jin Yook, "Natural convection around a radial heat sink", *International Journal of Heat and Mass Transfer*, Vol. 53, Issue 13-14, pp. 2935-2938, 2010.
- [8] R. Muwanga, I. G. Hassan, and M. Ghorab, "Numerical Investigation of a Radial Microchannel Heat Exchanger with Varying Cross-Sectional Channels", *Journal of Thermophysics and Heat Transfer*, Vol. 22, No. 3, pp. 321-332, 2008.
- [9] Pratanu Roy, N. K. Anand, and Debjyoti Banerjee, "A review of flow and heat transfer in rotating microchannels", *Procedia Engineering*, Vol. 56, pp. 7-17, 2013.
- [10] H. Ghaedamini, M. R. Salimpour, and A. Campo, "Constructal design of reverting microchannels for convective cooling of a circular disc", *International Journal of Thermal Sciences*, Vol. 50, Issue 6, pp. 1051-1061, 2011.
- [11] Shanglong Xu, Weijie Wang, Kuang Fang, and Chun-Nam Wong, "Heat transfer performance of a fractal silicon microchannel heat sink subjected to pulsation flow", *International Journal of Heat and Mass Transfer*, Vol. 81, pp. 33-40, 2015.
- [12] G. Hassan, R. Muwanga, and M. Ghorab, "Experimental study on heat transfer characteristics of microchannel system using liquid crystal thermography", Ph.D. Thesis, Mechanical and Industrial Engineering, Concordia University, 2007.
- [13] H. K. Versteeg, W. Malasekera, *An introduction to computational fluid dynamics (the finite volume method)*, Addison Wesley Longman Limited, 1995.
- [14] Andrei G. Fedorov and Raymond Viskanta, "Three-dimensional conjugate heat transfer in the microchannel heat sink for electronic packaging", *International Journal of Heat and Mass Transfer*, Vol. 43, Issue 3, pp. 399-415, 2000.

- [15] Sana J. Yaseen, Abul Muhsin A, Rageb, and Ahmed K. Alshara, "Thermal and fluid characteristics of three-layer microchannels heat sinks", *Invention Journal of Research Technology in Engineering & Management (IJRTEM)*, Vol. 1, Issue 12, pp. 61-70, 2017.
- [16] Deewakar Sharma, Harry Garg and P. P. Bajpai, "Performance Comparison of Single and Double Layer Microchannel Using Liquid Metal Coolants: A Numerical Study", *Arme*, Vol. 1, No. 2, pp. 9-17, 2012.

### Nomenclature

Symbol	Quantity	Unit (SI)
$A$	Area	$m^2$
$C_p$	Heat capacity	J/kg. K
$D_h$	Hydraulic diameter	m
$H$	Height	m
$k$	Thermal conductivity	W/m. K
$L$	Length	m
$\dot{m}$	Water mass flow rate	kg/s
$p$	Pressure	Pa
$q''$	Heat flux	W/m <sup>2</sup>
$r$	Radius	m
$T$	Temperature	K
$t$	Thickness	m
$u$	Fluid x-component velocity	m/sec
$v$	Fluid y-component velocity	m/sec
$w$	Fluid z-component velocity	m/sec
$W$	Width	m
$X$	Horizontal coordinate	m
$Y$	Vertical coordinate	m
$Z$	Axial coordinate	m
$\Delta P$	Pressure difference	Pa
$\Delta T$	Uniformity temperature	K

### Greek letters

Symbol	Quantity	Unit (SI)
$\rho$	Density	kg/m <sup>3</sup>
$\theta$	Channel angle	degree
$\beta$	Divergence angle of radial	degree
$\varphi$	Divergence angle of parallel	degree
$\alpha$	Aspect ratio	